

## MEASUREMENT OF FORWARD-SCATTER CROSS SECTIONS IN THE MELTING LAYER

F. G. Fernald and A. S. Dennis  
Stanford Research Institute

## 1. INTRODUCTION

The enhanced back-scatter from melting snowflakes compared to dry snow or rain of equivalent intensity gives rise to the well known bright band in the melting layer. Published computations by several authors, when considered together, indicate that forward-scatter cross sections in the melting layer occasionally exceed the back-scatter cross section by 1 to 2 orders of magnitude at centimeter wavelengths [Atlas *et al.*, 1953; Gunn and East, 1954; Herman and Battan, 1961; Stephens, 1961]. However, no complete theoretical treatment of scattering by melting snowflakes has been given to date because of their complex structures and irregular shapes. Therefore, an experiment was undertaken to obtain simultaneous determinations of forward-scatter and back-scatter cross sections in the melting layer.

## 2. EXPERIMENTAL SET-UP

The experiment was conducted in the vicinity of Sonora, California, in the western foothills of the Sierra Nevada near latitude 38 N. The propagation path was chosen so that the common volume (Fig. 1) was located near the melting layer during typical winter storms, and so that possible side-lobe and diffraction effects were minimized by the terrain.

A complete C-band weather radar was operated at the transmitter site. It transmitted 3- $\mu$ sec pulses of 250 kw peak power at 5.90 Gc at a pulse-repetition frequency of 333 per second. The antenna had an effective aperture of 0.5 m<sup>2</sup> and a pencil beam approximately 3.5° wide. The antenna-feed system permitted the use of either vertical or horizontal polarization. During the experiment, operations in sector-scan mode were alternated with periods during which the radar antenna remained fixed in the direction of the remote receiver. Photographs were taken of an auxiliary PPI display during the sector-scan operations to record precipitation areas along or near the propagation path. An A-scope, monitored visually, provided quantitative data on received power.

The remote receiver was built up from a marine radar, with the antenna mounted on its side. This arrangement produced a beam 15° wide in azimuth and 2° in the vertical. At the range of the common volume (~ 8 km), the vertical extent of the receiver beam approximated that of the bright band (Fig. 1). The receiver antenna was sensitive to vertically polarized radiation only. The output of the receiver was fed to 2 oscilloscopes, one serving as a monitor scope and the other being photographed.

## 3. METHOD OF ANALYSIS

Both the radar receiver and the remote receiver were calibrated with a test set during the course of the experiment. The calibration curves thus obtained provide a ready means for interpreting output voltages as shown on the oscilloscopes in terms of signal power at the antennas. However, further analysis is required before a direct comparison of forward-scatter and back-scatter cross sections is possible.

Figure 2 is a sample of the data recorded at the remote receiver. The oscilloscope was running on internal trigger with the horizontal writing speed at 1 cm/sec. The individual pulses are not resolved; the irregular trace is the envelope of the tops of the pulses. The fluctuations result from variations in the relative positions and (possibly) in the orientations of the particles in the common volume.

Mean signal intensities have been derived from records of the form of Fig. 2 using the threshold-crossing method described by Marshall and Hitschfeld [1953]. Let the threshold intensity be denoted by  $H$ , and the mean intensity at the remote receiver by  $\bar{P}_{rr}$ . If  $p$  instantaneous values of intensity out of a sample of  $k$  exceed  $H$ , the best estimate of  $\bar{P}_{rr}$  is given by

$$\tilde{P}_{rr} = \frac{H}{\log_e(k/p)} \quad (1)$$

Hard copy (HC) \$ 1.00

Microfiche (MF) \$ 0.50

174

FACILITY FORM 602

N65-19869  
(ACCESSION NUMBER)  
4  
(PAGES)  
CR-57468  
(NASA CR OR TMX OR AD NUMBER)

(THRU)

(CODE)

(CATEGORY)

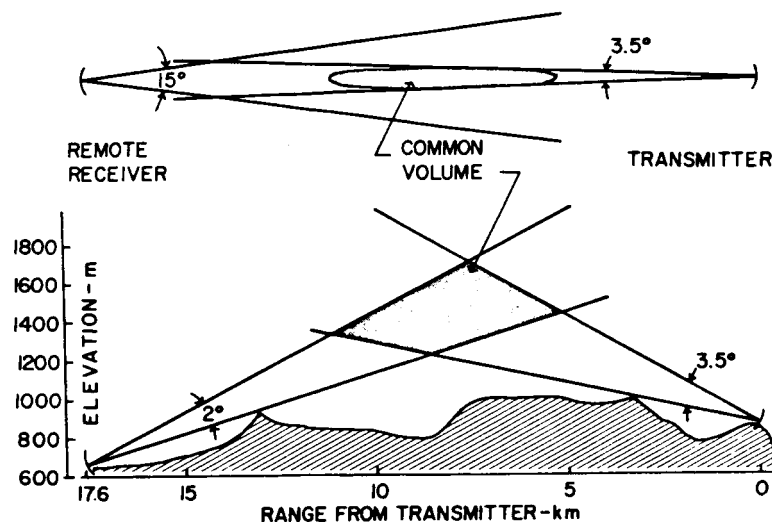


FIG. 1 PLAN AND PROFILE VIEWS OF PROPAGATION PATH

In our analysis, 100 instantaneous values of the signal envelope taken at 50 msec intervals have been used in each determination of  $\bar{P}_{rr}$ . If these were statistically independent and  $H$  were properly chosen, the errors in the estimate of  $\bar{P}_{rr}$  would be of the order of 1 db.

The autocorrelation of the signals at 50 msec intervals have been derived by noting the frequency of threshold crossings in the samples used to compute  $\bar{P}_{rr}$  [Hitschfeld and Dennis, 1956]. The coefficients range from 0.1 to 0.7, so that the ratio  $(T_{0.1}/\lambda)$ , where  $T_{0.1}$  is the time required for the autocorrelation coefficient to decrease to 0.1 and  $\lambda$  is the wavelength, ranges upward from  $10 \text{ msec cm}^{-1}$ . Thus, this ratio exceeds in every case the range of experimental values found for it by Hitschfeld and Dennis [1956] in analyzing back-scatter signals from snow. The relatively leisurely fluctuations in the forward-scatter signal are explainable on the basis of path geometry. In bistatic experiments involving small scattering angles, particle motions are very inefficient in producing changes in the total length of the path from transmitter to scatterer to receiver.

Due to the partial correlation of the instantaneous values of signal intensity used in the present case, each sample is equivalent to something less than 100 independent data, and so the standard error of our estimate of  $\bar{P}_{rr}$  is slightly greater than 1 db. However, it is estimated that measurement and calibration errors amount to upwards of 5 db, so the samples can be regarded as adequate for the present purpose.

The mean forward-scatter cross section per unit volume in the common volume,  $\eta_f$ , is given by

$$\eta_f = \frac{(4\pi)^3 \bar{P}_{rr} r^4}{P_t G_t G_r \lambda^2 V} \quad (2)$$

where  $r$  is one-half the length of the propagation path, i.e., 8.8 km,

$P_t$  is the transmitter power,

$G_t$  and  $G_r$  are the gains of the transmitting and receiving antennas,

$V$  is the common volume,

and the other symbols are as previously defined. In the present case (see Fig. 1), the common volume can be considered as the difference of 2 conical frustrums; geometrical construction shows it to be equal to  $0.5 \text{ km}^3$ .

The back-scatter cross section per unit volume at the middle of the common volume,  $\eta_b$ , is given by the weather radar equation as

$$\eta_b = \frac{8 \pi r^2 \bar{P}_r}{P_t A_e h} \quad (3)$$

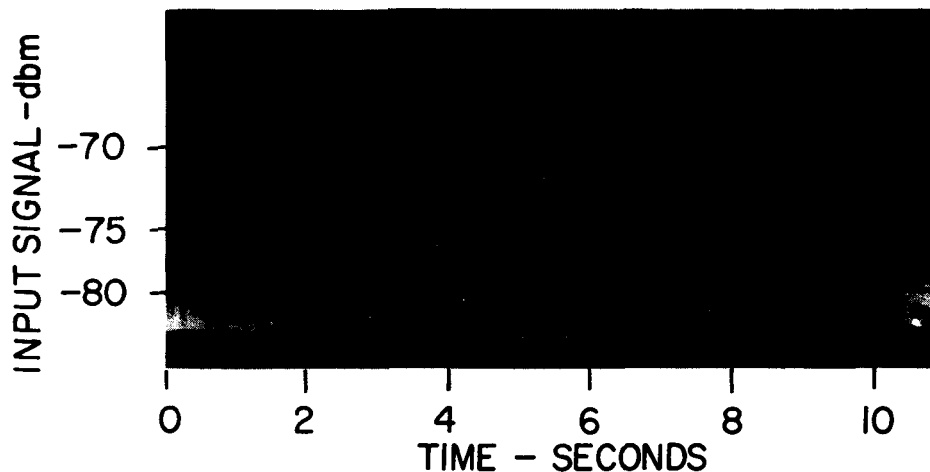


**FIG.2 FORWARD SCATTER SIGNAL RECORDED  
1327 PST, 1 APRIL 1964**

where  $P_r$  is the mean power collected at the radar antenna from a contributing region at range  $r$ ,  
 $A_e$  is the effective aperture of the radar antenna,  
 $h$  is the length of the radar pulse in space,  
and the other symbols are as previously defined.

#### 4. SAMPLE RESULTS AND CONCLUSIONS

Observations were conducted over a period of 7 weeks (19 February-9 April 1964). The storms during the first part of this period were rather cold, with dry snow occupying the common volume most of the time. Computed values of  $\eta_f$  and  $\eta_b$  in the dry snow were about the same when parallel polarization was used, but  $\eta_f$  was generally too small to be measured accurately when cross polarization was used.

The storm of 31 March-1 April 1964 proved ideal for bright-band measurements. At the start, the  $0^\circ$ -C isotherm was near 1.8 km, at the top of the common volume. Temperatures fell gradually throughout the storm, with the  $0^\circ$ -C isotherm dropping to 1.4 km by the end. At that time, the bright band was occupying the lower part of the common volume and extending perhaps 200 m below its lowest point.

Computed values of  $\eta_f$  and  $\eta_b$  are shown in Fig. 3. The PPI scope indicated quite uniform precipitation in the common volume during the late evening of 31 March, which is borne out by the relatively steady values of  $\eta_f$  and  $\eta_b$ . A preponderance of forward scatter is indicated, with  $\eta_f$  as high as  $-68 \text{ db m}^{-1}$  and exceeding  $\eta_b$  by 6 to 15 db.

During the morning of 1 April, numerous small showers with diameters of 1 to 3 km were present along and near the propagation path. The function  $\eta_b$  fluctuated widely, but  $\eta_f$  did not because the common volume was large enough to hold several precipitation cells at once (Fig. 3). Scattering was predominantly forward. If it had been isotropic,  $\eta_b$  would have exceeded  $\eta_f$  at 1110 PST when one of the showers passed through the middle of the common volume.

Cross-polarized measurements were made from 1205 to 1300 PST. They coincided with the passage of a large shower of moderate intensity, which probably contained some small hail. The values of  $\eta_f$  ranged from 0-10 db below  $\eta_b$ , indicating that they were 10-25 db below the corresponding values of  $\eta_f$  for parallel polarization. This is compatible with Wexler's [1955] results on back-scattered signals from the melting layer.

Parallel-polarized measurements around 1330 PST, as the last showers were moving off the path, showed  $\eta_f$  only slightly in excess of  $\eta_b$ . The value of  $\eta_f$  at 1402 PST,  $-100 \text{ db m}^{-1}$ , was contributed either by precipitation at the edge of the common volume of the main beams or in sidelobes.

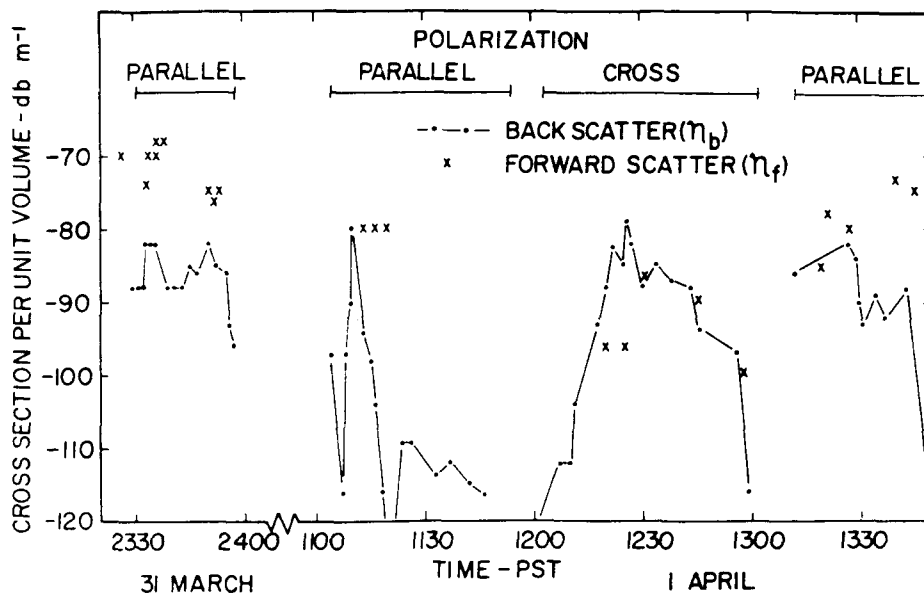


FIG. 3 CALCULATED CROSS SECTIONS PER UNIT VOLUME

The results obtained, although limited for the most part to one storm, do confirm the expectation that  $\eta_f$  should exceed  $\eta_b$  in the bright band at centimeter wavelengths. Further experimentation is needed to establish the range of the ratio  $\eta_f/\eta_b$ . It would be advantageous if such experiments provided for simultaneous measurements of the parallel-polarized and cross-polarized forward-scatter signals.

#### 5. ACKNOWLEDGMENTS

This work was sponsored by the National Aeronautics and Space Administration under Contract NASr-49(02) with Stanford Research Institute.

Mr. R. T.H. Collis, Head of the Institute's Radar Aerophysics Group played a major role in the planning of the field operations. Quite extensive equipment modifications were necessary in converting surplus radar sets for this experiment. This work was handled by Mr. G. E. Davis, Senior Electronics Technician.

#### 6. REFERENCES

- Atlas, D., M. Kerker and W. Hitschfeld (1953), Scattering and Attenuation by Non-Spherical Atmospheric Particles, *J. Atmos. and Terrest. Phys.*, Vol. 3, pp. 108-119.
- Gunn, K. L. S., and T. W. R. East (October 1954), Microwave Properties of Precipitation Particles, *Quart. J. Royal Meteorol. Soc.*, Vol. 80, pp. 525-545.
- Herman, B. M., and L. J. Battan (1961), Calculations of the Total Attenuation and Angular Scatter of Ice Spheres, *Proc. Ninth Weather Radar Conference*, Kansas City, Missouri, pp. 259-265, Amer. Meteorol. Soc., Boston, Massachusetts.
- Hitschfeld, W., and A. S. Dennis (July 1956), Measurement and Calculation of Fluctuations in Radar Echoes from Snow, *Sci. Report MW-23*, Contract AF-19(122)-217, McGill University, Montreal, Quebec.
- Marshall, J. S., and W. Hitschfeld (1953), Interpretation of the Fluctuating Echo from Randomly Positioned Scatterers: Part I, *Canadian J. Phys.*, Vol. 31, pp. 962-995.
- Stephens, J. J. (June 1961), Radar Cross Sections for Water and Ice Spheres, *J. Meteorol.*, Vol. 18, pp. 348-359.
- Wexler, R. (1955), An Evaluation of the Physical Effects in the Melting Layer, *Proc. Fifth Weather Radar Conf.*, pp. 329-334, Signal Corps Engineering Laboratories.